

## Canalization of subwavelength images by electromagnetic crystals

Pavel A. Belov and Constantin R. Simovski

*Photonics and Optoinformatics Department, St. Petersburg State University of Information Technologies, Mechanics and Optics, Sablinskaya 14, 197101, St. Petersburg, Russia*

Pekka Ikonen

*Radio Laboratory, Helsinki University of Technology P.O. Box 3000, FIN-02015 HUT, Finland*

(Received 4 February 2005; published 31 May 2005)

The original regime of operation for flat superlenses formed by electromagnetic crystals is proposed. This regime does not involve negative refraction and amplification of evanescent waves in contrast to the perfect lenses formed by left-handed media. The subwavelength spatial spectrum of a source is canalized by the eigenmodes of the crystal having the same longitudinal components of wave vector and group velocities directed across the slab. The regime is implemented at low frequencies with respect to the crystal period by using capacitively loaded wire media. The resolution of  $\lambda/6$  is demonstrated. The thickness of the superlens is not related with the distance to the source and the lens can be made thick enough.

DOI: 10.1103/PhysRevB.71.193105

PACS number(s): 42.25.Fx, 41.20.Jb, 42.70.Qs

The theoretical possibility of subwavelength imaging by a slab of left-handed medium<sup>1</sup> (LHM) with  $\varepsilon = \mu = -1$  was demonstrated by Pendry in his seminal work.<sup>2</sup> The focusing phenomenon in Pendry's perfect lens is based on two effects. The propagating modes of a source are focused in the LHM due to the negative refraction and the evanescent modes experience amplification inside the LHM slab. This allows one to restore subwavelength details in the focal plane. The second effect happens due to the resonant excitation of the surface plasmons at the interfaces of the slab. To the present time the LHM is created only for frequencies up to 1 THz.<sup>3</sup> It is an ambitious goal to obtain the subwavelength resolution without LHM in the optical frequency range. In this range the negative refraction phenomenon is observed in photonic crystals<sup>4</sup> at frequencies close to the band gap edges. This fact was theoretically revealed by Notomi<sup>5</sup> and experimentally verified by Parimi *et al.*<sup>6</sup> A flat *superlens* formed by a slab of photonic crystal was suggested by Luo *et al.* in Ref. 7 and the possibility of subwavelength imaging was theoretically studied in Ref. 8. The experimental verification of the imaging effect was demonstrated in Ref. 9. We use the term superlens for a layer of an artificial material which transports the subwavelength images into the far zone of the source. The principle of Luo's superlens is similar to the principle of Pendry's perfect lens: negative refraction for propagating modes and amplification due to the resonant surface plasmon for evanescent modes. Both effects are obtained without left-handed properties of a material. Negative refraction is obtained due to a specific form of isofrequency contours (without backward waves inherent to LHM). The further increase of the resolution for Luo's superlens can be achieved simultaneously increasing the dielectric permittivity of the host medium, and decreasing the lattice period.<sup>8</sup> In practice, this is not a helpful way in optical frequency region where large permittivity for real media is related with high losses. Also, an important factor deteriorating the image is the finite thickness of the superlens. The eigenmodes excited in the crystal experience multiple reflections from the interfaces and their interference disturbs the image. This destructive interference

appears due to the mismatch between wave impedances of air and photonic crystal, and is inevitable for some angles of incidence. In the case of Pendry's perfect lens this defect is avoided because left-handed medium with  $\varepsilon = \mu = -1$  is matched with air for all angles of incidence. Luo *et al.* in Ref. 7 partially solved the problem with matching by choosing an appropriate thickness of the slab. In this case the slab operates as a Fabry-Perot resonator. However, this solution is not complete since the Fabry-Perot resonance holds only for a narrow range of incidence angles.

In the present Brief Report we solve the problems described above. For that purpose we suggest to use the photonic crystal in a different regime than suggested by Luo *et al.* in Ref. 7. We do not involve negative refraction and amplification of evanescent modes, rather, we propose to transform the most part of the spatial spectrum of the source radiation into propagating eigenmodes of the crystal having practically the same group velocity (directed across the slab) and the same longitudinal components of the wave vector. The spatial harmonics produced by a source (propagating and evanescent) refract into the crystal eigenmodes at the front interface. These eigenmodes propagate normally to the interface and deliver the distribution of near-field electric field from the front interface to the back interface without disturbances. The incoming waves refract at the back interface and form an image. This way the incident field with subwavelength details is transported from one interface to the other one. We will call the described regime canalization with subwavelength resolution.

The similar regimes for propagating spatial harmonics are called self-guiding,<sup>10</sup> directed diffraction,<sup>11</sup> self-collimation,<sup>12</sup> and tunneling.<sup>13</sup> One can see from the results of Refs. 11–13 that the canalization dominates over negative refraction in the superlens suggested in Ref. 7. However, in these papers the canalization for evanescent harmonics was not noticed. It allows one to avoid the negative refraction at all while obtaining the superlens and achieve subwavelength resolution. In fact, the canalization has the similar principle of operation as the medium with zero re-

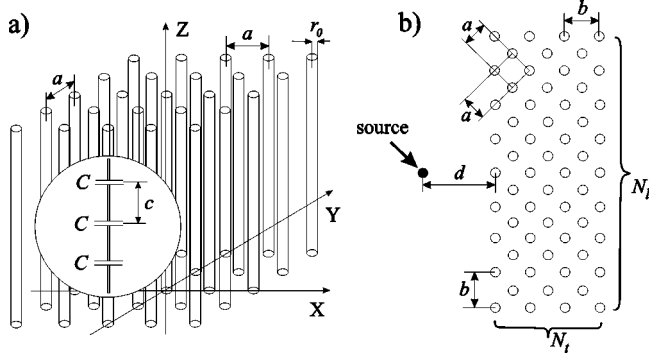


FIG. 1. (a) Geometry of capacitively loaded wire medium (CLWM); (b) Geometry of the flat lens formed by CLWM.

fraction index.<sup>14</sup> The difference is that in our case the image is transmitted by waves which all vary identically with distance from the front interface, whereas in zero refraction index medium there is no such variation. Also, the similar effect is observed in bilayers of media with indefinite permittivity and permeability tensors<sup>15</sup> where the pair of layers effectively compensate the properties of each other and provides total transmission within wide range of the transverse wave vectors.

The problem of strong reflection from a slab can be solved by choosing its thickness appropriately so that it operates as a Fabry-Perot resonator. In our case the Fabry-Perot resonance holds for all incidence angles and even for incident evanescent waves. The reason is that after the refraction all these waves acquire the same longitudinal component of the wave vector for which the Fabry-Perot resonator is tuned. Thus, in our regime the superlens does not suffer the image deterioration due to its finite thickness, because there are no waves traveling along the interfaces. Moreover, we suppose that the proposed regime helps to avoid the problems related to finite transverse size of the lenses inherent to LHM slabs.<sup>16</sup>

The regime of canalization can be implemented by using the isofrequency contour which has a rather long flat part. Such contours are available for different types of photonic crystals. In the present study we use a two-dimensional electromagnetic crystal formed by capacitively loaded wires<sup>17</sup> [see Fig. 1(a)], the so-called capacitively loaded wire medium (CLWM). We have chosen this type of the crystal since the analytical result for the dispersion properties of the infinite CLWM is available,<sup>17</sup> and the finite size samples of CLWM with large numbers of loaded wires can be easily numerically analyzed.<sup>18</sup> Other types of electromagnetic crystals (such as photonic crystals with high dielectric permittivities of components<sup>7,8</sup>) can be applied as well, but their studies will require additional efforts.

The CLWM has a band gap near the resonant frequency of a single capacitively loaded wire.<sup>17</sup> The position of this band gap (the so-called resonant band gap) can be tuned by changing the value of the load capacitance. The high value of capacitance allows to locate the resonant band gap at much lower frequencies than the first lattice resonance.<sup>17</sup> This way it is possible to obtain band gap at very low frequencies without increasing the dielectric permittivity of the host me-

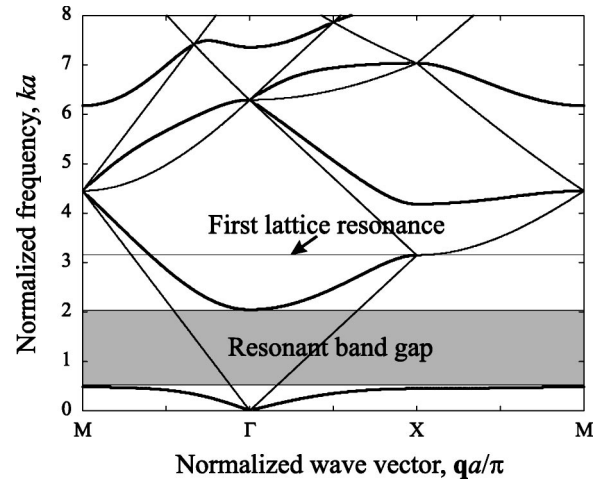


FIG. 2. Dispersion diagram for CLWM.

diuum. Note, that this resonant band gap has the same nature as band gap caused by resonant properties of a component material.<sup>19,20</sup>

The typical dispersion diagram for CLWM is presented in Fig. 2.  $k$  is the wave number of host media.  $\Gamma = (0, 0, 0)^T$ ,  $X = (\pi/a, 0, 0)^T$ ,  $Y = (0, \pi/a, 0)^T$ , and  $M = (\pi/a, \pi/a, 0)^T$  are points in the first Brillouin zone. The parameters of the structure normalized by lattice period  $a$  are the following: radius of wires  $r_0 = 0.058a$ , period of loading  $c = 0.55a$  and loading capacitance  $C = 2\text{pF}$ .

The isofrequency contours for the frequency region near the lower edge of the resonant band gap are shown in Fig. 3. The isofrequency of the host medium is shown as the small circle around  $\Gamma$  point. The variation of this circular contour radius is negligible over the interval of normalized frequency  $ka = 0.46 \cdots 0.474$ .

According to the Luo's approach<sup>7,8</sup> one should tune the isofrequency contours of the host medium and the crystal (located around points  $\Gamma$  and  $M$ , respectively) to have the same form. For that purpose one should use the frequency  $ka = 0.474$  (see Fig. 3). In this case the propagating waves would negatively refract and the evanescent part of the spa-

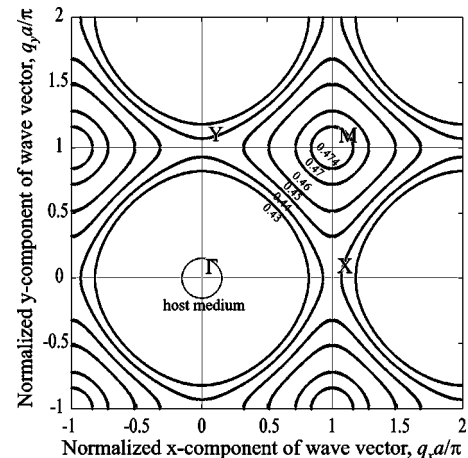


FIG. 3. Isofrequency contours for CLWM. The numbers correspond to values of  $ka$ .

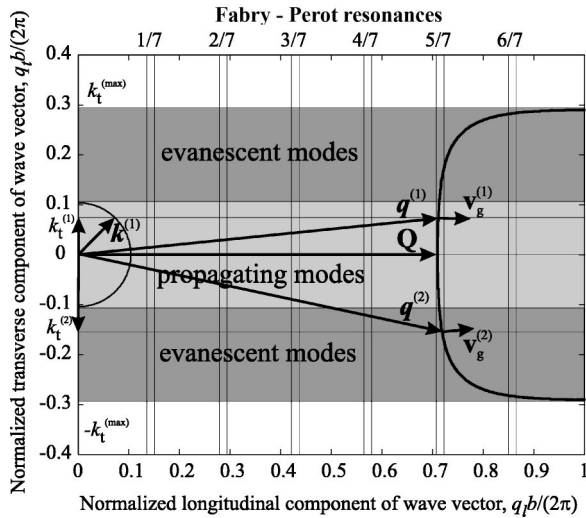


FIG. 4. Isofrequency contours for the canalization regime.

tial spectrum would excite the surface plasmons. This regime leads to the strong reflection from the interfaces which cannot be completely damped by the Fabry-Perot resonance. We cannot obtain the subwavelength resolution for CPWM in this regime.

The part of the isofrequency contour of the crystal corresponding to  $ka=0.46$  and located within first Brillouin zone is practically flat. This part is perpendicular to the diagonal of the first Brillouin zone. Thus, in order to achieve canalization regime we orient interfaces of the slab orthogonally to the (11) direction of the crystal as shown in Fig. 1(b). As a result, we obtain the situation shown in Fig. 4, where the isofrequency contours corresponding to  $ka=0.46$  are plotted in terms of longitudinal  $q_l$  (with respect to the interfaces) and transversal  $q_t$  components of the wave vector.

The circle at the left side of Fig. 4 is the isofrequency contour of the host medium and the curve at the right side is the part of CLWM isofrequency contour corresponding to the propagation from the left to the right. We denote the wave vector of CLWM eigenmode with  $q_t=0$  as  $\mathbf{Q}$  and introduce notation  $k_t^{\max}=\sqrt{2\pi/a-Q}$ . All propagating spatial harmonics of a source and the wide range of evanescent ones refract into the eigenmodes with longitudinal wave vector close to  $\mathbf{Q}$ . There is a part of the isofrequency contour with  $|k_t| \approx k_t^{\max}$  which is not flat but it corresponds to the very narrow band of evanescent wave spectrum and we neglect its contribution. The light shaded region ( $|k_t| \leq k$ ) in Fig. 4 corresponds to the propagating incident waves. The dark shaded regions ( $k < |k_t| \leq k_t^{\max}$ ) correspond to the evanescent incident waves which transform into the propagating eigenmodes after refraction. The refraction of the propagating wave with  $k_t=k_t^{(1)}$ ,  $|k_t^{(1)}| < k$  and the evanescent wave with  $k_t=k_t^{(2)}$ ,  $k < |k_t^{(2)}| \leq k_t^{\max}$  is illustrated in Fig. 4. Both waves refract (keeping the transverse wave vector component) into the eigenmodes which have longitudinal wave vectors close to  $\mathbf{Q}$  and practically identical group velocities ( $\mathbf{v}_g^{(1)}$  and  $\mathbf{v}_g^{(2)}$ ) directed across the slab. Though the transversal components of the wave vector are retained in the refraction ( $q_t=k_t$ ), this does not mean the transversal propagation of refracted

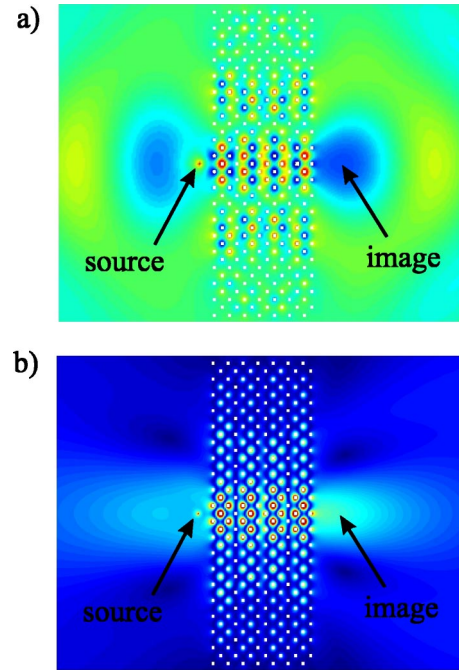


FIG. 5. Distribution of electric field amplitude (a) and intensity (b),  $ka=0.46$ ,  $N_l=14$ ,  $N_t=39$ .

waves. These components describe the transversal phase distribution of the waves traveling across the slab (this is similar to the so-called transmission-line modes of wire media<sup>21</sup>).

The condition of the Fabry-Perot resonance is  $QN_l b/2 = m\pi$ , where  $N_l$  is number of the crystal planes along the longitudinal direction of the slab [see Fig 1(b)],  $m$  is the number of half wavelengths and  $b/2=a/\sqrt{2}$  is the longitudinal distance between the layers. In our case  $N_l=14$  layers of CLWM (or any multiple of 14) allows to satisfy the Fabry-Perot resonance condition. The regions corresponding to Fabry-Perot resonances are shown in Fig. 4 and vector  $\mathbf{Q}$  lies within the fifth region ( $m=5$ ). This choice allows one to achieve transmission coefficient equal to unity practically for all spatial harmonics with transverse component of wave vector within the band  $[-k_t^{\max}, k_t^{\max}]$ . Thus, we can estimate the value of transverse size  $\Delta$  for the image of the point source with help of Eq. (11) of Ref. 8. This estimation gives  $\Delta=2\pi/k_t^{\max}=3.4b$ .

The result of numerical simulation for excitation of the slab by a point source located at the distance  $d=b=\sqrt{2}a$  from front interface  $a$  [see Fig. 1(b)] is presented in Fig. 5. The image near the back interface is observed. The transverse size of the image (found from the intensity distribution using the Rayleigh criterium) turns out to be  $\Delta=3.4b$ , which exactly coincides with the theoretical estimation. This size is only about 70% higher than the ultimate resolution limit  $\Delta=2b$  obtained in Ref. 8. Moreover, we deal with the subwavelength resolution, because the radius of the focal spot is  $\Delta/2=1.7b \approx \lambda/6$ . We conclude that the canalization allows transportation of the subwavelength images from one interface to the other. Though the imaging can be achieved only with the sources which are located closely enough to the front interface, the utilization of our regime is advantageous compared to the Pendry's perfect lens. Our lens can be made

thick, since its required thickness is not related with the distance  $d$  to the source. It is practically important for the near-field microscopy in the optical range, when the needle of the microscope used as a probe can be located physically far from the tested source. Then we can avoid the destruction of the sources under testing by the microscope and can prepare a mechanically solid superlens.

The canalization regime offers an attractive possibility for transportation of subwavelength images. The main requirement for that purpose is the flatness of some part of an isofrequency contour. We have demonstrated that such contours are available for CLWM at microwaves. In the optical range the similar contours are available for photonic crystals with high permittivity.<sup>7,8</sup> Both samples operate for  $s$ -polarized incident waves. For the  $p$ -polarized waves there is another possibility to obtain flat isofrequency contour in a material. Moreover, one can obtain an isofrequency perfectly flat and infinitely long. Recently, we have studied simple unloaded wire medium (WM) from electromagnetic crystal point of view.<sup>21</sup> WM has been known for a long time as an artificial dielectric with negative permittivity at low frequencies. Our studies revealed the strong low-frequency spatial dispersion in such a media. This effect appears to be due to the transmission-line modes (TL modes) of such a crystal. The lens formed by a slab WM is presented in Fig. 6. The TL modes have TEM polarization and travel across the slab (along wires) with wave vector which has longitudinal component  $q_l$  equal to  $k$  and arbitrary transverse component  $q_t$ . In terms of isofrequency contour it means that WM has a flat isofrequency contour for all values of transverse component of wave vector. If we choose the thickness of the slab as a multiple of half-wavelength we obtain the Fabry-Perot resonator. This slab has transmission coefficient equal to unity for any  $p$ -polarized incident wave (propagating or evanescent) with any transverse component of wave vector. The WM lens principle of operation is very simple. The front interface transforms incident field into TL modes which are all identically transmitted to the back interface (as with the

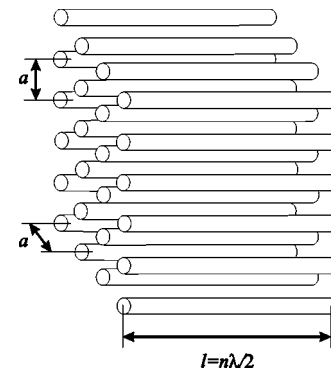


FIG. 6. Geometry of the flat lens formed by wire medium.

usual TEM transmission line). Thus, the lens from WM canalizes  $p$ -polarized near field of the source.<sup>22</sup> For  $s$ -polarized incident waves the slab operates practically as the host medium because the transverse polarization of thin wires is negligibly small. This situation is opposite to the case of the lens formed by CLWM, which canalizes  $s$ -polarized field, but operates as the host medium for  $p$ -polarized incident wave. Both WM and CLWM superlenses can be made as thick as it is necessary to make the testing of the near-field images appearing on their back interfaces practically feasible. In our example of the CLWM, the required number of layers is a multiple of 14. The WM superlens should have the thickness equal to the integer number of half wavelengths.

We have suggested a regime of the near-field image transportation from the front interface to the back interface of a photonic crystal layer. This canalization regime can be realized at frequencies much lower than the frequency of the lattice resonance using capacitively loaded wire media. We have shown subwavelength resolution with transverse size of the focal spot equal to  $\lambda/3$ . This result can be further improved by increasing the value of loading capacitance in order to decrease operational frequency with respect to frequency of the first lattice resonance.

<sup>1</sup>V. Veselago, *Sov. Phys. Usp.* **10**, 509 (1968).

<sup>2</sup>J. B. Pendry, *Phys. Rev. Lett.* **85**, 3966 (2000).

<sup>3</sup>T. J. Yen, W. J. Padilla, N. Fang, D. C. Vier, D. R. Smith, J. B. Pendry, D. N. Basov, and X. Zhang, *Science* **303**, 1494 (2004).

<sup>4</sup>K. Sakoda, *Optical Properties of Photonic Crystals* (Springer-Verlag, Berlin, 2001).

<sup>5</sup>M. Notomi, *Phys. Rev. B* **62**, 10696 (2000).

<sup>6</sup>P. V. Parimi, W. T. Lu, P. Vodo, J. Sokoloff, J. S. Derov, and S. Sridhar, *Phys. Rev. Lett.* **92**, 127401 (2004).

<sup>7</sup>C. Luo, S. G. Johnson, J. D. Joannopoulos, and J. B. Pendry, *Phys. Rev. B* **65**, 201104(R) (2002).

<sup>8</sup>C. Luo, S. G. Johnson, J. D. Joannopoulos, and J. B. Pendry, *Phys. Rev. B* **68**, 045115 (2003).

<sup>9</sup>P. V. Parimi, W. T. Lu, P. Vodo, and S. Sridhar, *Nature (London)* **426**, 404 (2003).

<sup>10</sup>D. N. Chigrin, S. Enoch, C. M. S. Torres, and G. Tayeb, *Opt. Express* **11**, 1203 (2003).

<sup>11</sup>H.-T. Chien, H.-T. Tang, C.-H. Kuo, C.-C. Chen, and Z. Ye, *Phys.*

*Rev. B* **70**, 113101 (2004).

<sup>12</sup>Z.-Y. Li and L.-L. Lin, *Phys. Rev. B* **68**, 245110 (2003).

<sup>13</sup>C.-H. Kuo and Z. Ye, *Phys. Rev. E* **70**, 056608 (2004).

<sup>14</sup>R. W. Ziolkowski, *Phys. Rev. E* **70**, 046608 (2004).

<sup>15</sup>D. R. Smith and D. Schurig, *Phys. Rev. Lett.* **90**, 077405 (2003).

<sup>16</sup>L. Chen, S. He, and L. Shen, *Phys. Rev. Lett.* **92**, 107404 (2004).

<sup>17</sup>P. A. Belov, C. R. Simovski, and S. A. Tretyakov, *Phys. Rev. E* **66**, 036610 (2002).

<sup>18</sup>C. Simovski and S. He, *Microwave Opt. Technol. Lett.* **31**, 214 (2001).

<sup>19</sup>A. Moroz, *Phys. Rev. Lett.* **83**, 5274 (1999).

<sup>20</sup>P. A. Belov, S. A. Tretyakov, and A. J. Viitanen, *Phys. Rev. E* **66**, 016608 (2002).

<sup>21</sup>P. A. Belov, R. Marques, S. I. Maslovski, I. S. Nefedov, M. Silverininha, C. R. Simovski, and S. A. Tretyakov, *Phys. Rev. B* **67**, 113103 (2003).

<sup>22</sup>S. Maslovski (private communication).